Spatiotemporal patterns of terrestrial carbon cycle during the 20th century

Shilong Piao,[1,2] Philippe Ciais,[2] Pierre Friedlingstein,[2] Nathalie de Noblet-Ducoudré,[2] Patricia Cadule,[2] Nicolas Viovy,[2] and Tao Wang[1,2]

Received 21 August 2008; revised 28 June 2009; accepted 31 July 2009; published 20 November 2009.

[1] We evaluated how climate change, rising atmospheric CO_2 concentration, and land use change influenced the terrestrial carbon (C) cycle for the last century using a process-based ecosystem model. Over the last century, the modeled land use change emitted about 129 Pg of C to the atmosphere. About 76% (or 98 Pg C) of this emission, however, was offset by net C uptake on land driven by climate changes and rising atmospheric CO_2 concentration. Thus, the modeled net release of C from the terrestrial ecosystems to the atmosphere from 1901 to 2002 is about 31 Pg C. Global net primary productivity (NPP) has significantly increased by 14% during the last century, especially since the 1970s. From 1980 to 2002, global NPP increased with an average increase rate of 0.4% yr^{-1}. At global scale, such an increase seems to be primarily attributed to the increase in atmospheric CO_2 concentration, and then to precipitation change. Over the last 2 decades, climate change and rising CO_2 forced the land carbon sink (1.6 Pg C yr^{-1} for 1980s and 2.2 Pg C yr^{-1} for 1990s) to be larger than land use change driven carbon emissions (1.0 Pg C yr^{-1} for 1980s and 1.2 Pg C yr^{-1} for 1990s), resulting a net land sink of 0.5 Pg C yr^{-1} in the 1980s and of 1.0 Pg C yr^{-1} in the 1990s. The largest C emission from land use change appeared in tropical regions with an average emission of 0.6 Pg C yr^{-1} in 1980s and 0.7 Pg C yr^{-1} in 1990s, which is slightly larger than net carbon uptake due to CO_2 fertilization and climate change. Thus, net carbon balance of tropical lands is close to neutral over the past 2 decades (about 0.13 Pg C yr^{-1} in 1980s and 0.03 Pg C yr^{-1} in 1990s). We also found that current global warming has already started accelerating C loss from terrestrial ecosystems, by enhanced decomposition of soil organic carbon. In response to warming trends only, the global net carbon uptake significantly decreased, offsetting about 70% of the increase in global net carbon uptake owing to CO_2 fertilization during 1980–2002. The global terrestrial C cycle also shows large year-to-year variations, and different regions have quite distinct dominant drivers. Generally, interannual changes of carbon fluxes in tropical and temperate ecosystems are mainly explained by precipitation variability, while temperature variability plays a major role in boreal ecosystems.

Citation: Piao, S., P. Ciais, P. Friedlingstein, N. de Noblet-Ducoudré, P. Cadule, N. Viovy, and T. Wang (2009), Spatiotemporal patterns of terrestrial carbon cycle during the 20th century, *Global Biogeochem. Cycles*, *23*, GB4026, doi:10.1029/2008GB003339.

1. Introduction

[2] Terrestrial ecosystems play an important role in the global carbon (C) cycle due to the large amount of C storage and the large magnitude of the gross fluxes of C exchanged with the atmosphere. Even a small shift in each gross flux may result into a great change in the net carbon balance of terrestrial ecosystems, and thus affect the future atmospheric CO_2 concentration curve and global climate [*Cox et al.*, 2000; *Friedlingstein et al.*, 2006]. Previous studies indicated that over the last several decades, global terrestrial ecosystems acted as net carbon sinks, taking up 2–4 Pg C yr^{-1}, and accounting for 10–60% of the C emitted through human activities [*IPCC*, 2007]. Monitoring and understanding these patterns and processes in the terrestrial C cycle is critically important because it will help us not only to more accurately predict its behavior in the future, but also to determine the reasonable goal of reducing fossil fuel emissions.

[3] Climatic factors exert direct controls on the terrestrial C exchange with the atmosphere primarily through the balance between photosynthesis, respiration and fire disturbances [*Houghton*, 2000; *Schaefer et al.*, 2002]. Although it

[1]Department of Ecology, College of Urban and Environmental Science, Peking University, Beijing, China.
[2]LSCE, UMR CEA, CNRS, Gif-sur-Yvette, France.

0886-6236/09/2008GB003339$12.00

Table 1. Description of Simulations Used in This Study

Simulation	CO_2	Climate	Land Use Change	Fire
S1	Yes	Yes	No	Yes
S2	Yes	No	No	Yes
S3	No	Yes, but only temperature	No	Yes
S4	No	Yes, but only precipitation	No	Yes
S5	Yes	Yes	No	No
S6	Yes	Yes	Yes	No

is well known that rising temperature will increase the growing season length and promote vegetation productivity in the middle and high latitudes of the Northern Hemisphere [*Lucht et al.*, 2002; *Fang et al.*, 2003], the effects of current temperature change on the terrestrial C balance have not been adequately quantified [*Piao et al.*, 2008], because rising temperature also accelerates C loss through soil decomposition [*Rustad et al.*, 2001; *Davidson and Janssens*, 2006; *Kirschbaum*, 2000]. Net uptake of carbon occurs where gains due to increased vegetation growth outweigh soil C losses and disturbances. Changes in precipitation amount and distribution also significantly alter current regional-scale and global-scale terrestrial C cycles [*Churkina and Running*, 1998; *Ciais et al.*, 2005; *Fang et al.*, 2005]. Previous observation analyses and simulation models both found a net abnormal source of CO_2 from tropical ecosystems during the El Niño phase of El Niño–Southern Oscillation (ENSO), which is known to increase dry season length and decrease wet season rainfall in tropical region [e.g., *Keeling et al.*, 1995; *Behrenfeld et al.*, 2001; *Jones et al.*, 2001; *Rodenbeck et al.*, 2003; *Zeng et al.*, 2005].

[4] Land use change is the major disturbance that can alter terrestrial carbon storage and fluxes, and can have a particularly long-term impact on the terrestrial carbon cycle at regional and global scales [*Gitz and Ciais*, 2003; *Sitch et al.*, 2005]. Generally, when forests are cleared for cultivation or pasture, the carbon contained in the living material and soil is released to the atmosphere, but the regrowth of forests on abandoned agricultural land will cause the sequestration of carbon [*Vuichard et al.*, 2008]. The carbon losses from land use changes are generally quicker than the recovery of carbon stocks [*Arrouays et al.*, 2002]. Over the past three centuries, there has been a net loss of 12×10^6 km^2 of forest and woodlands to cropland, and about half that amount of grasslands, savannas, and steppes to cropland [*Ramankutty and Foley*, 1999]. Such large-scale changes in land cover have been suggested to be responsible for a large portion of the human induced increase in atmospheric CO_2 [*McGuire et al.*, 2001; *Houghton*, 2003; *Jain and Yang*, 2005], but there are large uncertainties due to lack of detailed information on the land use change [*DeFries et al.*, 2002; *Houghton*, 2007].

[5] During the past decades, considerable efforts have been made to improve our knowledge about the separate effects of climate, atmospheric CO_2 and land use change on terrestrial C cycle. However, the mechanisms and factors that govern the uptake and release of C from the terrestrial reservoir, and their regional importance, are still poorly quantified because long-term in situ measurements are very sparse, and remote sensing techniques are only partially effective [*Valentini et al.*, 2000; *IPCC*, 2007]. There have already been several C cycle modeling studies for understanding and predicting global terrestrial carbon cycle [*McGuire et al.*, 2001; *Cao et al.*, 2002; *Zeng et al.*, 2005; *Peylin et al.*, 2005], but most of them have not separated the contribution of change in temperature and change in precipitation to global carbon balance. In this study, we use a process-based C cycle model, Organizing Carbon and Hydrology in Dynamic Ecosystems (ORCHIDEE) [*Krinner et al.*, 2005] to quantify the effects of changes in climate, atmospheric CO_2 concentration and changes in land cover area on terrestrial C cycle for the period from 1901 to 2002. Since most deforestation occurs in forests with a very long natural fire return interval, and ORCHIDEE does not separate between forests prone to fire and moist forests which never burn in each pixel, fire disturbance was not activated in the simulations S5 and S6 used to calculate the land use flux (Table 1). A central goal of the study is to investigate the temporal and spatial variability of terrestrial C cycle over the last century and to separately identify the relative contributions of different factors.

2. Methods

2.1. ORCHIDEE Model

[6] The ORCHIDEE model [*Krinner et al.*, 2005] is a dynamic global vegetation model (DGVM) representing key vegetation processes governing terrestrial biogeochemistry and biogeography. In this study, however, we switched off vegetation dynamic simulation module since there are large uncertainties in DGVM modeled vegetation distribution [*Krinner et al.*, 2005; *Sitch et al.*, 2008]. ORCHIDEE distinguishes 12 plant functional types with different photosynthetic, phenological and morphological characteristics. Plant CO_2 assimilation in ORCHIDEE model is based on work by *Farquhar et al.* [1980] for C3 plants and *Collatz et al.* [1992] for C4 plants. Maintenance respiration is a function of each living biomass pool and temperature, while growth respiration is computed as a fraction of the difference between assimilation inputs and maintenance respiration outputs to plant biomass. According to the resource balance hypothesis and optimal allocation theory [*Friedlingstein et al.*, 1999], plants adjust C allocation among leaves, stem and roots in a way that balances resource acquisition (e.g., carbon, nutrients, and water). Heterotrophic respiration parameterization is taken from CENTURY [*Parton et al.*, 1988], while a simple parameterization of fire follows *McNaughton et al.* [1989] and *Sitch et al.* [2003].

[7] The current version of ORCHIDEE takes into account the effects of land use change on terrestrial C cycle. For each year, the fractions of each land use type are updated annually. With changes in natural vegetation, a specified amount of C contained in heartwood and sapwood aboveground are transferred to three product pools with different turnover times (1 year, 10 years, and 100 years), while the C contained in other biomass pools (leaves, roots, sapwood belowground, fruits and heartwood aboveground) is added to litter reservoir and eventually released to the atmosphere through decomposition. The fraction of C assigned to each product reservoir depends on vegetation types, and the rate

of decay for each product pool does not vary through time. Following *McGuire et al.* [2001], 59.7%, 40.3%, and 0% of harvest heartwood and sapwood aboveground biomass for the tropical vegetation (tropical broad leaved evergreen forest, tropical broad leaved raingreen forest, and C4 grass) was assigned to the product decay pools with 1 year, 10 year, and 100 year turnover times, respectively, while 59.7%, 29.9%, and 10.4% ratios were applied to temperate and boreal vegetation types. In the case of cropland abandonment, corresponding natural vegetation is allowed to regrow in the area of abandoned land.

[8] Crop carbon cycle is disturbed by human activity more intensely than that of other natural vegetation. Unlike natural vegetation, for instance, parts of crop production are harvested and consumed by humans directly. Independent of crop types, the fraction of annual NPP (FANPP) consumed by humans ranges from 0.25 to 0.85 [*Hicke and Lobell*, 2004]. The value of FANPP was set to 0.45 in this study. In addition, several studies have shown that anthropogenic factors, such as tillage, generally accelerate soil organic C decomposition rate [*Murty et al.*, 2002; *Buyanovsky and Wagner*, 1998], and the magnitude of this effect may also vary among crop management activities. In this study, the effect of cultivation on crop soil C decomposition rate is considered through simply multiplying the decomposition rate in each pool by a cultivation factor like in the CENTURY model [*Parton et al.*, 1988], where the cultivation factor was set to be 1.1 for drill, 1.3 for sweep, row-cultivator and rodweeder, and 1.6 for ploughing and cultivator. Lacking information on historic changes in spatial distribution of cultivation techniques, the cultivation factor in our current simulation is set to be spatially constant, but dependent on crop types. We take a higher value of 1.3 for C4 crops and a lower value of 1.1 for C3 crops. This is because most C4 crops are mainly distributed in tropical regions where generally more than one crop per year grow. It should be also noted that ORCHIDEE does not represent accurately cultivated plants and the farming practices impacting their growth. However, these processes missing may be not significantly influence the accuracy of land use change caused global C emission estimation because of the lack of historical information on the spatial patterns of cultivated plants and farming practices. The parameterization of C process for pastureland is simply treated as nature grassland.

[9] ORCHIDEE has been extensively validated against observed seasonal cycles of energy and water exchanges and C fluxes at various eddy-covariance sites and, through the use of an atmospheric transport model, against the seasonal and interannual variability of atmospheric CO_2 concentration at globally distributed atmospheric sites [*Krinner et al.*, 2005; *Ciais et al.*, 2005; *Piao et al.*, 2008]. Spatio-temporal change in leaf area index (LAI) derived from ORCHIDEE is also compared with that in satellite-observed greenness indexes from 1982 to 2002 [*Krinner et al.*, 2005; *Piao et al.*, 2006], showing that the modeled phenology captures the observed interannual and decadal greenness trends well. The ORCHIDEE simulated response of NBP (Net Biome Production) to future climate change and rising CO_2 concentration is intermediate among five DGVM which were compared by *Sitch et al.* [2008]. These former studies suggest a potential applicability of the model for exploring historical terrestrial C cycle dynamics.

2.2. Data Sets

[10] The meteorological data used to run ORCHIDEE include air temperature, precipitation, wet day frequency, diurnal temperature range, cloud cover, relative humidity of the air, and wind speed. Monthly data sets, with a spatial resolution of $0.5^\circ \times 0.5^\circ$ for 1901–2002, were supplied by the Climatic Research Unit (CRU), School of Environmental Sciences, University of East Anglia, United Kingdom [*Mitchell and Jones*, 2005]. Since wind speed data are only available starting 1960, we used the average wind speed data during the period 1960–2002 in our historical simulation from 1901 to 2002. In other words, wind speed data are not changed during the whole study period. Since the climate forcing in ORCHIDEE was defined at a half-hourly time step, weather generator algorithms were employed to disaggregate monthly climate variables into half-hourly. For precipitation, the occurrence of wet or dry days and daily precipitation amount were determined from monthly precipitation, with wet day frequency from a Richardson-type weather generator [*Richardson and Wright*, 1984]. Daily precipitation amounts were converted to half-hourly by evenly distributing rainfall throughout the day. For temperature, daily minimum (Tmin) and maximum values (Tmax) were approximated from mean monthly air temperature and diurnal temperature range through multivariate generation models conditioned on the wet or dry status of the day according to *Richardson* [1981]. Half-hourly temperature are then generated from daily values of Tmin and Tmax by using a sine wave assuming that maximum temperature occurs at 14:00 local time and minimum temperature occurs at sunrise [*Campbell and Norman*, 1998]. Daily surface pressure was calculated on the basis of the function of daily temperature and elevation, and the constant value was assumed throughout the day. Following the approximation of daily wind speed values from monthly means by linear interpolation, half-hourly wind speed were calculated by a logarithmic function of both daily value and independent random number generated from the normal distribution [*Nicks et al.*, 1990]. For specific humidity, monthly relative humidity derived from monthly vapor pressure was linearly interpolated to daily values, which were further calibrated conditioned on the wet or dry status of the day [*Nicks et al.*, 1990]. The daily specific humidity can thus be obtained from air temperature and relative humidity. The approach implemented in generating half-hourly specific humidity values from daily is the same as for air temperature mentioned above. Half-hourly downwelling shortwave radiation under clear sky condition was calculated on the basis of solar zenithal angle, depending on the hour, the day of year and latitude. It is then modulated by daily cloud cover (obtained from the monthly fields in the same way as daily temperature) based on the linear regression parameters from *Friend* [1998].

[11] Cropland area from 1860 to 1992 is prescribed each year from the data set of *Ramankutty and Foley* [1999]. We have combined this data set with that of *Goldewijk* [2001] to account for the changing extent of pasture from 1860 to 1992. The distribution of natural vegetation at each grid cell is derived from *Loveland et al.* [2000]. The extent of natural

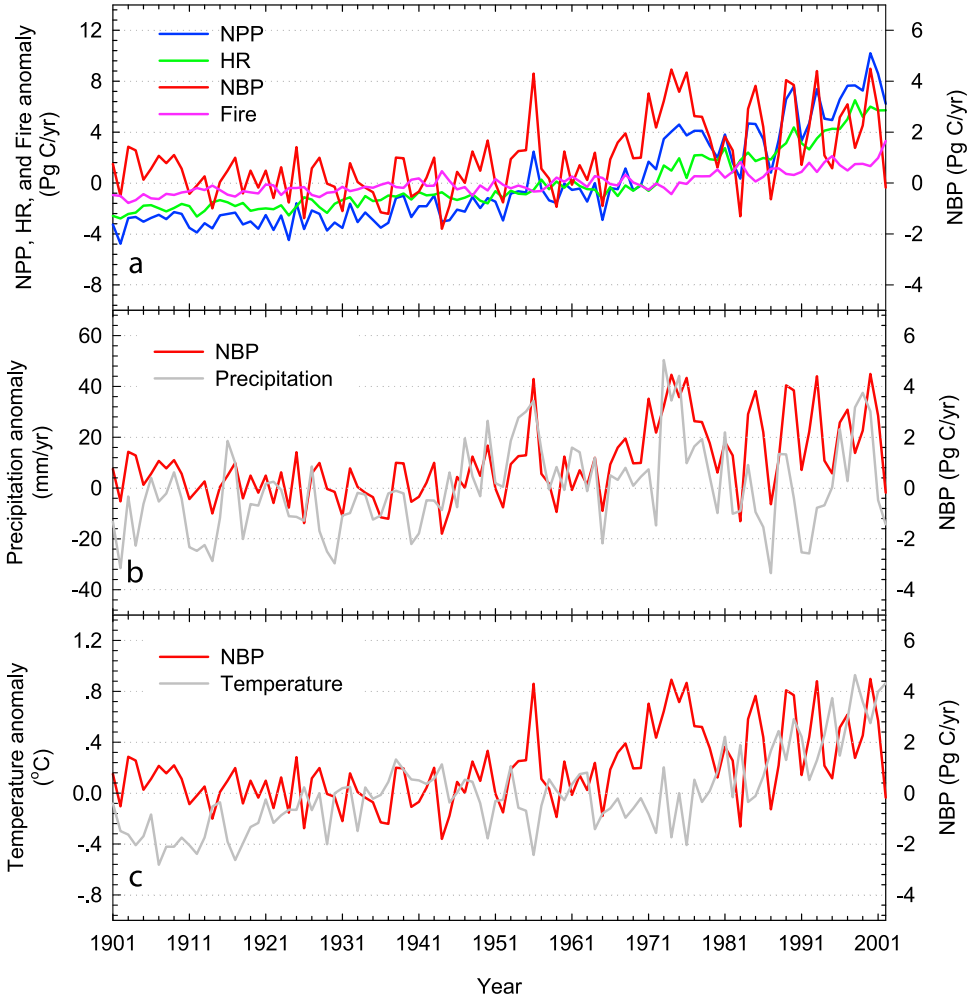

Figure 1. Changes in anomalies of total terrestrial net primary productivity (NPP, Pg C yr^{-1}), heterotrophic respiration (HR, Pg C yr^{-1}), nature fire-induced carbon (C) emission (Pg C yr^{-1}), total terrestrial net biome productivity (NBP, Pg C yr^{-1}), anomalies of annual precipitation (mm), and anomalies of annual mean temperature (°C) from 1901 to 2002. C flux is derived from simulation S1 which only considers climate change and rising atmospheric CO_2. The averages of global total NPP, HR, and fire emission from 1901 to 2002 are 70 Pg C yr^{-1}, 65 Pg C yr^{-1}, and 4 Pg C yr^{-1}, respectively. Positive values of NBP indicate carbon sinks, and negative values of NBP indicate carbon sources.

vegetation varies with time as a function of the prescribed extent of cropland and pasture. Changes in crop and pasture extent from 1992 till 2002 is derived from the IMAGE 2.2 scenarios (http://www.mnp.nl/image/image_products/). We use an anomaly procedure to ensure consistency between both data sets. Detailed description on this data set is given by N. de Noblet-Ducoudré et al. (2008, http://www.cnrm.meteo.fr/ensembles/public/data/LandUseMaps_Informations.pdf).

3. C Balances Associated With Changes in Climate and CO_2 Over the Last Century

[12] In this section, we analyze the climate change driven interannual variation of C flux over the last century. To do so, we first integrated the model at a resolution of 2° × 2° for about 1000 years until the C pools reach equilibrium (less than 0.01% year to year C storage change) based on transient climate data during the period 1901–1910 and the 1860 atmospheric CO_2 concentration of 286.05 ppm. The model was then run until 1900 with the variable climate of the period 1901–1910 and the corresponding atmospheric CO_2 concentration data during 1860–1900. This state was used as the initial condition for the last century simulation (S1) which only considered climate change and rising atmospheric CO_2 (Table 1).

3.1. Global C Balance

[13] Figure 1 shows the interannual variability and trends in modeled global annual NPP, heterotrophic respiration (HR), fire emissions, and resulting net C balance (NBP). The variability of NBP is also compared to the one of temperature and precipitation from 1901 to 2002 (Figures 1b and 1c). Global annual NPP and HR significantly increased during the last century, especially since the 1970s. The

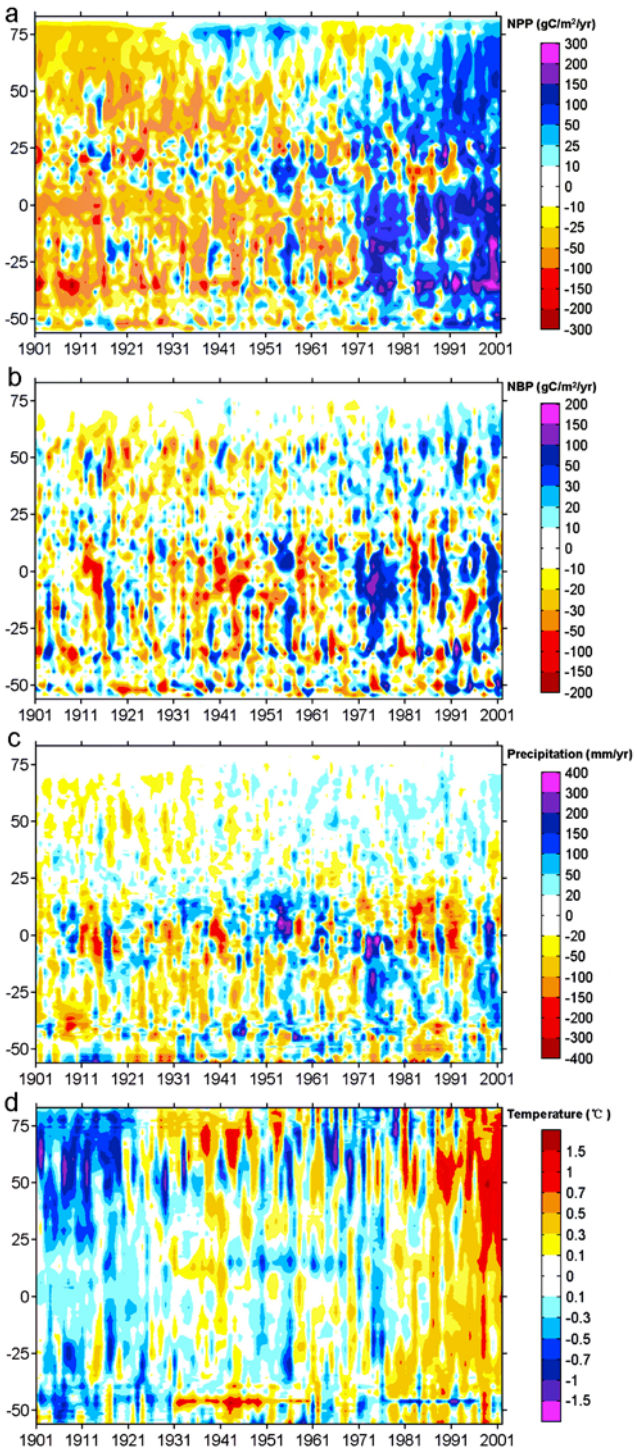

Figure 2. Interannual variation in anomalies of annual NPP (g C m^{-2} yr^{-1}), annual NBP (g C m^{-2} yr^{-1}), anomalies of annual precipitation (mm yr^{-1}), and anomalies of annual temperature (°C) at different latitudes from 1901 to 2002. C flux is derived from simulation S1 which only considers climate change and rising atmospheric CO_2. Positive values of NBP represent carbon uptake, and negative values of NBP represent carbon release.

global annual NPP increased from 67.5 Pg C yr^{-1} in 1901 to 77.0 Pg C yr^{-1} in 2002, a total increase of 14.1% or an average rate of 0.11 Pg C yr^{-1}. Annual NBP fluctuated around 0 during 1901–1970, while often showed positive values (sink) during the following 3 decades because of the rapidly increasing vegetation productivity (Figure 1).

[14] Interannual variations in global NBP lockstepped more closely those in NPP ($R^2 = 0.58$; $P < 0.001$) than those in HR ($R^2 = 0.27$, $P < 0.001$) and fire ($R^2 = 0.02$, $P = 0.12$), implying that, in ORCHIDEE, the variations in terrestrial net C balance are primarily determined by the variations in vegetation productivity (as observed by *Law et al.* [2006]). In terms of climate effects, variations in global NBP are best explained by variations in precipitation, in agreement with earlier studies [*Schaefer et al.*, 2002]. For example, the "hump" in terrestrial net C uptake during the period 1973–1975 was anomalously large (3.7 ± 0.6 Pg C yr^{-1}), is strongly linked with abnormally high NPP (4.0 ± 0.6 Pg C yr^{-1}) caused by above-average precipitation (43 ± 8 mm yr^{-1}). In contrast, substantially low precipitation was observed in 1914, 1930, 1940, 1965, and 1987, leading to a corresponding large C loss from terrestrial ecosystems in these years.

3.2. Spatial Patterns of the Interannual Variations in C Balance

[15] The interannual variations in modeled NPP and NBP at different latitudes are illustrated in Figure 2. In comparison to the early last century, NPP during the last 2 decades have significantly increased at nearly all latitudes, except in the latitude strip of 5–15°N, where NPP showed persistent negative anomalies (<−50 gC m^{-2} yr^{-1}) during the 1980s. The drought stress due to a dramatic decrease in precipitation (Figure 2c) is likely responsible for the reduced vegetation productivity during that period in these regions. On the other hand, the modeling results show that patterns of NPP changes correspond closely with temperature changes over the high-latitude region (north of 50°N). For instance, vegetation productivity north of 50°N was abnormally high (>10 gC m^{-2} yr^{-1}) during the periods 1940–1960 and 1980–2000, which is associated with abnormally high temperature (Figure 2d). Conversely, likely due to temporary cooler temperatures, NPP significantly decreased in the 1960s and 1970s across the high-latitude belt.

[16] There is a large variability in the magnitude and sign (sink or source) of NBP from year to year, in response to climate anomalies. As shown by Figure 2b, carbon losses from tropical ecosystems have been abnormally strong (<−50 gC m^{-2} yr^{-1}) in warm and dry years, such as 1914, 1930, 1940, 1965, 1983, and 1987, whereas wetter and cooler years were significantly correlated with an increase in net C uptake (e.g., 1917, 1956, 1973–1975, 1985, 1989, and 2000).

[17] In order to analyze both spatial and temporal variability of land C fluxes driven by climate, an empirical orthogonal function (EOF) analysis was conducted for NPP and NBP in the early (period 1901–1920) and late (period 1980–1999) 20th century. The results suggest that time evolution (principal component) of the first EOF component of both NPP and NBP is significantly related with the interannual variation of monthly Southern Oscillation Index (SOI), particularly with SOI for January ($R^2 = 0.28$, $P <$

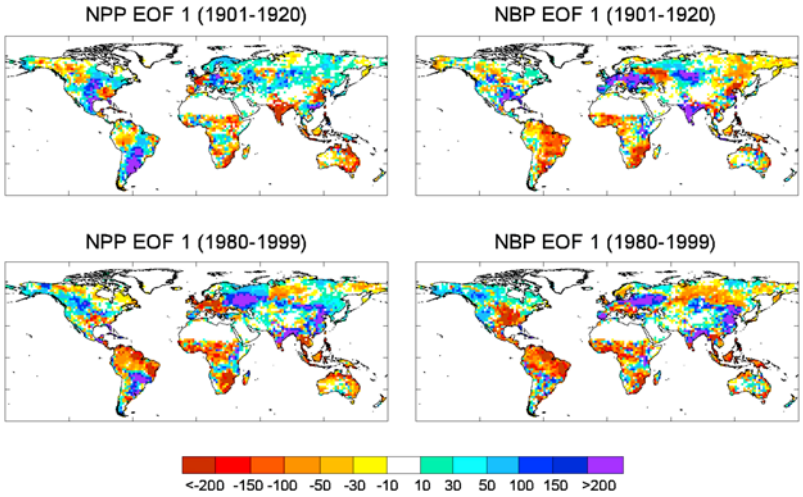

Figure 3. Spatial patterns of the first empirical orthogonal function (EOF) component from EOF analysis of NPP and NBP derived from simulation S1 which only counts climate change and rising atmospheric CO_2 during the periods 1901–1920 and 1980–1999.

0.05 for NPP; $R^2 = 0.19$, $P < 0.05$ for NBP), February ($R^2 = 0.52$, $P < 0.05$ for NPP; $R^2 = 0.34$, $P < 0.05$ for NBP), and March ($R^2 = 0.24$, $P < 0.05$ for NPP; $R^2 = 0.16$, $P < 0.05$ for NBP). The spatial patterns of the first EOF component of NBP is close to that of NPP, particularly in the late 20th century, further suggesting that variation in NBP is primarily regulated by variation NPP (Figure 3). Similar to previous analysis by *Zeng et al.* [2005], the spatial patterns of the first EOF component of NPP and NBP generally mirrored C flux anomalies during El Niño events (Figure 4), indicating that ENSO forced changes in climate are the dominant mechanism explaining the variability in NPP and NBP during the last century. In the southeastern United States, southeastern South America, eastern Europe, and eastern China however, the first EOF component of NBP is negatively correlated with the El Niño pattern. In comparison with the early 20th century, the spatial patterns of positive abnormal NBP seem to have moved northward over America (Figure 3).

3.3. Characteristic Response of C Balance to ENSO

[18] In order to further explore the spatial patterns of ENSO effects on terrestrial C balance, we first calculated the anomalies of NPP and NBP in 1989, the strongest La Niña event on record, and in 1998, the strongest El Niño event, relative to the 9 year means over the period surrounding each event by ±4 years.

[19] It is well known that precipitation decreases over the most of tropical region during El Niño episodes and increases during La Niña episodes [*Jones et al.*, 2001]. In addition, generally significant increase in temperature was also observed during El Niño episodes [*Hashimoto et al.*, 2004]. In response to El Niño in 1998, the modeled NPP is strongly decreased over the Amazon (<-100 gC m^{-2} yr^{-1}), the savannas region and eastern equatorial forests in Africa (-100–-50 gC m^{-2} yr^{-1}), in the eastern United States and in South Asia (<-100 gC m^{-2} yr^{-1}) due to drought, while there is an increase of NPP in the eastern parts of China (>150 gC m^{-2} yr^{-1}), India (>100 gC m^{-2} yr^{-1}), and over most of western and northern North America (>30 gC m^{-2} yr^{-1}) (Figure 4b). Similar patterns are observed from satellite-derived NDVI data sets from *Tucker et al.* [2005] (Figure 4d) in most of regions except in the eastern Amazon basin and Indonesia, which may be related to cloud effects on satellite greenness [*Slayback et al.*, 2003]. As shown in Figure 4f, the terrestrial biosphere functions as a net source of CO_2 to the atmosphere during the major El Niño event of 1998, particularly in the tropical regions (<-50 gC m^{-2} yr^{-1}) and eastern North America (<-50 gC m^{-2} yr^{-1}). An opposite regional response compared to El Niño is found for La Niña events in the modeled NPP and NBP (Figures 4a–4b and 4e–4f), except in central and eastern Europe and in European Russia and western Siberia, where both La Niña and El Niño coincide with a drop in NPP and an abnormal source for NBP. The same direction of changes in NBP of these regions during both El Niño in 1998 and La Niña in 1989 suggests that regional C flux changes are not significantly affected by ENSO [*Schaefer et al.*, 2002].

4. Changes in Terrestrial C Balance Forced by Changes in Climate and CO_2 From 1980 to 2002

[20] As shown in Figures 1 and 2, the period from 1980 to 2002 saw the most rapid increase in NPP of the 20th century. In this section we focus in more detail on the attribution of this NPP trend to the forcing of atmospheric CO_2, temperature, and precipitation for the period 1980–2002. To do so, we performed new sensitivity simulations (S2, S3, and S4) by varying only one driving variables during 1980–2002 (Table 1). S1 simulation–derived state in 1979 is used as initial conditions for the simulation of S2, S3 and S4. In simulation S2, only atmospheric CO_2 is varied, and climate variables in 1979 are used during the whole 1980–2002 period. In simulation S3, only temperature is varied, and in simulation S4, only precipitation is varied. The effects of other climate variables other than temperature and precip-

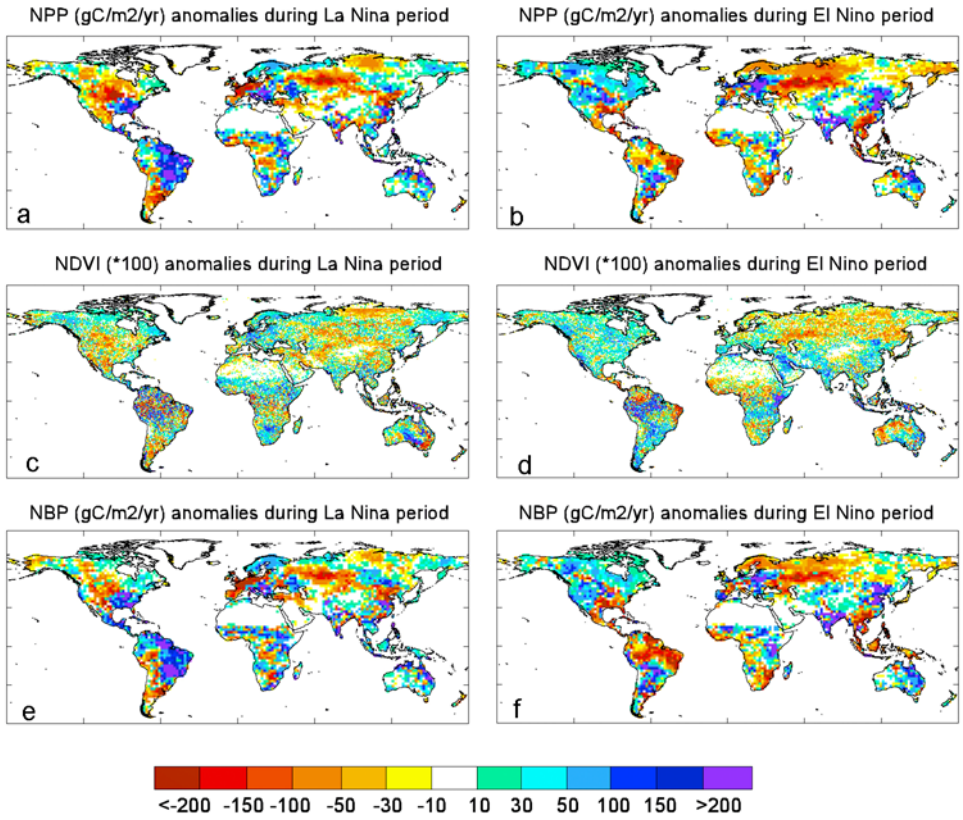

Figure 4. Spatial patterns of modeled NPP, NBP, and satellite-derived annual NDVI anomalies in El Niño years (1998) and La Niña years (1989). NBP is derived from simulation S1 which only considers climate change and rising atmospheric CO_2. Annual NDVI is defined as sum of bimonthly NDVI which is lager than 0.1.

itation are evaluated by subtracting the sum of S2, S3 and S4 from the previous simulation (S1) where all forcing variables are varied. Finally, the individual contribution of each factor (atmospheric CO_2, temperature, and precipitation) to the trend in C fluxes is defined as the ratio of the linear flux trend over 1980–2002 derived from each sensitivity simulation (S2, S3, and S4, respectively) to that of simulation S1.

4.1. Attributing the Global Trends in NPP and NBP

[21] Simulation S1 predicted that global NPP has increased from 74.3 Pg C yr^{-1} in the early 1980s (average of 1980–1982) to 80.3 Pg C yr^{-1} in the early 2000s (average of 2000–2002) with a linear trend of 0.3 Pg C yr^{-2} or 0.4% yr^{-1} (Figure 5). Such a significant increase of NPP seems to be primarily attributed to the increase in atmospheric CO_2 concentration (contributing 0.24 Pg C yr^{-2} or 80% of the NPP linear trend), and then by precipitation trend to wetter conditions (0.07 Pg C yr^{-2}). Conversely, rising temperature alone is modeled to cause a weak negative trend in global NPP (−0.02 Pg C yr^{-2}). On the other hand, interannual changes in global NPP in simulation S1 are most significantly correlated with those in simulation S4 where only precipitation varies ($R = 0.84$, $P < 0.001$). This suggests that at global scale, rainfall variability is the dominant control of NPP interannual variability in ORCHIDEE, whereas it is less important in controlling NPP trends over the past 2 decades.

[22] For global NBP, our results suggest that global warming has already begun to accelerate global C loss (Figure 5). In response to rising temperature alone, global NBP has significantly decreased by 0.05 Pg C yr^{-1} ($P < 0.05$), which is about 70% of increase in NBP driven by rising atmospheric CO_2 concentration (0.07 Pg C yr^{-1}; $P < 0.05$). Overall, the simulation S1 modeled global NBP varies between 1.3 Pg C yr^{-1} in 1983 and −4.5 Pg C yr^{-1} in 2000, with a slight increase in the sink of 0.05 Pg C yr^{-2} over the past 2 decades (Figure 5). The interannual variability of global NBP in simulation S1 matches most closely with that in simulation S4 which only considers precipitation changes ($R = 0.88$, $P < 0.001$), further indicating that year-to-year variation in global NBP is mainly driven by precipitation variation, just as for NPP. However, it should be noted that the large, anomalous, negative, climate-driven NBP anomaly (net C emission, simulation S1) in 1998 is due to the significant increase in global temperature, consistent with previous studies [e.g., *Erbrecht and Lucht*, 2006].

4.2. Spatial Patterns of NPP and NBP Trends

[23] Figure 6a displays the spatial distribution of the linear NPP trend from 1980 to 2002 (simulation S1). The largest NPP positive trend (over 5.0 gC m^{-2} yr^{-2}) is seen

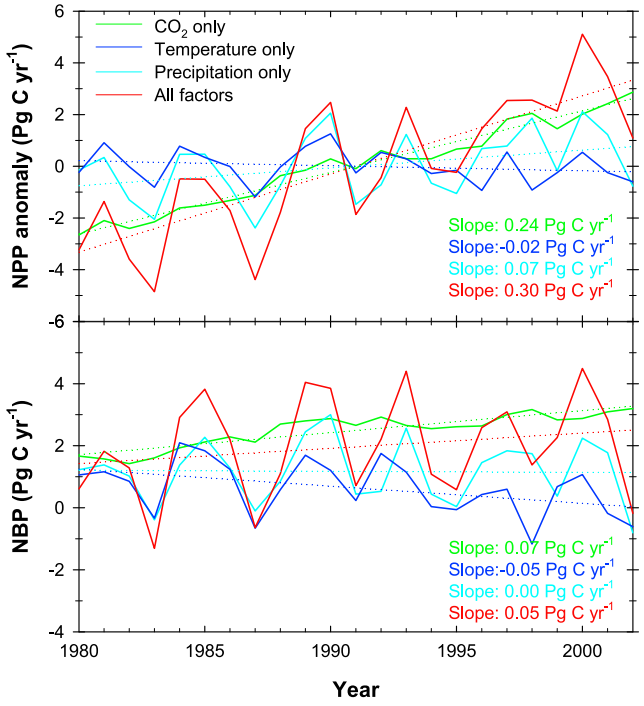

Figure 5. Interannual changes in anomalies of global total NPP (Pg C yr^{-1}) and total NBP (Pg C yr^{-1}) estimated from simulations S1 (considered both atmospheric CO_2 and climate variability), S2 (only considered CO_2 increase), S3 (only considered temperature change), and S4 (only considered precipitation change) from 1980 to 2002. Positive values of NBP represent carbon uptake, and negative values of NBP represent carbon release.

over the central United States, the La Plata basin in South America, Guyana, Sahelian, Sudanese and southern African savannas, southern European Russia, southwestern China, the maritime continent and northern Australia. In contrast, southwestern United States, northeastern China, most of eastern Europe and the Great Lakes region in Africa show a persistent negative trend of NPP (Figure 6a). Overall, NPP increased over 80% of the ecosystems, indicating a dominant rise in productivity during the last 2 decades.

[24] Due to substantially enhanced vegetation productivity, the largest increase in carbon sink in simulation S1 is found in central United States, central Africa, western Russia, maritime continent and northern Australia, with a linear trend of over 3.0 gC m^{-2} yr^{-2} (Figure 6b). Only a few areas mostly experience a dramatic decrease in NBP over the last 2 decades. These regions with decreasing NBP are broadly similar with those of decreasing NPP (Figure 6a).

[25] A summary of ORCHIDEE-derived NPP and NBP trend different forcing factors in four different regions is presented in Figure 7. All regions show significant increasing trend of NPP in simulation S1, but relative contributions of different factors are not constant (Figure 7). The CO_2 fertilization effects (simulation S2) are the major cause for the increase of NPP in tropical region (114 Tg C yr^{-2}) (between 20°S and 20°N) and northern temperate region (63 Tg C yr^{-2}) (between 20°N and 50°N) where a decreasing trend of annual NPP (−7 Tg C yr^{-2}) occurs in simulation S3 that only considered the effects of temperature variability, indicating that the recent warming alone does not benefit vegetation growth in this region. In the Southern Hemisphere (south of 20°S) and the boreal region (north of 50°N), the contribution from climate change is comparable to that from CO_2 fertilization effects.

[26] The insignificant decrease in annual NBP (16 Tg C yr^{-2}) obtained in simulation S1 is found in northern temperate region where in response to solely current temperature change, net C uptake significantly decreased at the rate of 23.6 Tg C yr^{-2} ($R = 0.54$, $P < 0.05$), which offsets the increase in sink caused by rising atmospheric CO_2 concentration (15.2 Tg C yr^{-2}). The modeled net C uptake of tropical (35 Tg C yr^{-2}) and boreal regions (18 Tg C yr^{-2}) is enhanced during the last 2 decades, and CO_2 fertilization effects are primarily responsible for this enhancement (32 Tg C yr^{-2} and 17 Tg C yr^{-2}, respectively). In addition, precipitation change also contributed to the increase in carbon sink in the Southern Hemisphere (4.6 Tg C yr^{-2}) and tropical region (13.8 Tg C yr^{-2}).

4.3. Impacts of Climate Change on the Interannual Variability in C Flux

[27] Figure 8 shows the spatial distribution of climatic controls on the interannual variability in NPP and NBP derived from the S1 simulation (considering all factors) over the last 2 decades. The explained variability caused by each climatic factor (temperature, precipitation, and other climate

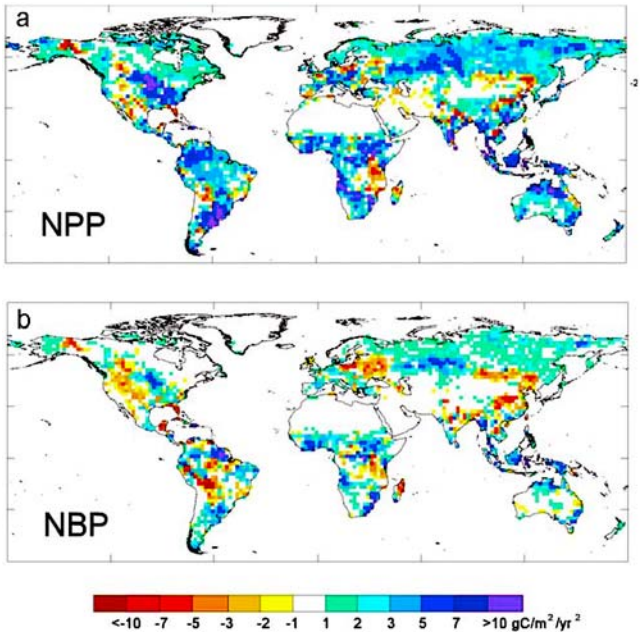

Figure 6. Spatial distribution of the trends in annual (a) NPP and (b) NBP derived from simulation S1 (considered both atmospheric CO_2 and climate variability) from 1980 to 2002. The trends were calculated on the basis of linear regression of C fluxes with year using ordinary least squares. Positive values of NBP indicate increasing net carbon uptake.

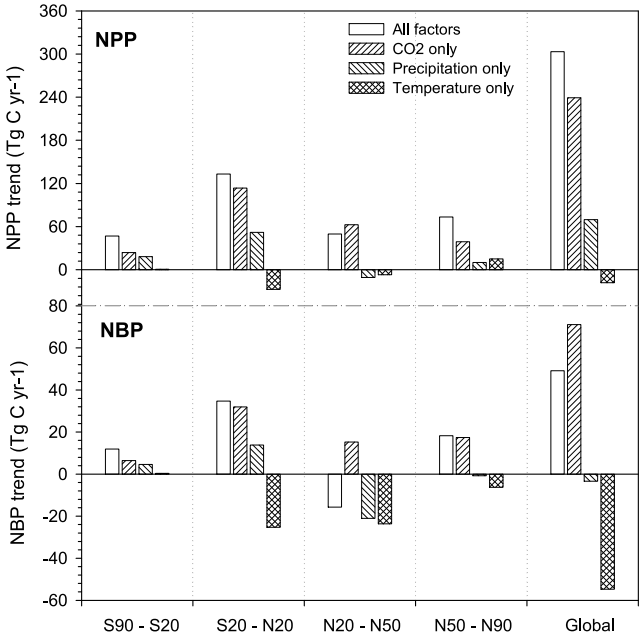

Figure 7. Trends of total NPP and total NBP for different regions estimated by simulations S1 (considered both atmospheric CO_2 and climate variability), S2 (only considered CO_2 increase), S3 (only considered temperature change), and S4 (only considered precipitation change) from 1980 to 2002. Positive values of NBP indicate increasing net carbon uptake.

factors) is assessed through calculating the square of temporal correlation coefficients between C fluxes derived from each corresponding simulation (S3, S4, and S1 – S2 – S3 – S4, respectively) to that from simulation S1.

[28] As shown in Figure 8a, temporal changes in NPP in high-latitude regions and Tibet are mainly explained by temperature changes, while precipitation variations are the major driving variable accounting for NPP variations in most other regions, except western Amazonian forests where the contributions from different climatic factors are also significant (radiation limited photosynthesis). These different controls on NPP are expected since northern ecosystems and Tibet are rather cold and rarely water limited, while most other regions are warmer and relatively more water limited [*Reichstein et al.*, 2007]. In the northeastern part of Siberian region, our results show that other climate factors than temperature and precipitation are primarily responsible for the interannual variations in vegetation productivity (explaining more than 50% of the total variance in NPP). Cloud cover change may exert significant control over the interannual variability in NPP in this region, mainly through influencing light availability for plant growth.

[29] Similar patterns of controlling drivers are also observed in NBP (Figure 8b), but the temperature explained variation of NBP in boreal regions is somewhat weaker than that of NPP. This may be attributed to the parallel positive responses of NPP and HR to temperature change. Overall, in more than 70% of global vegetation surface, precipitation

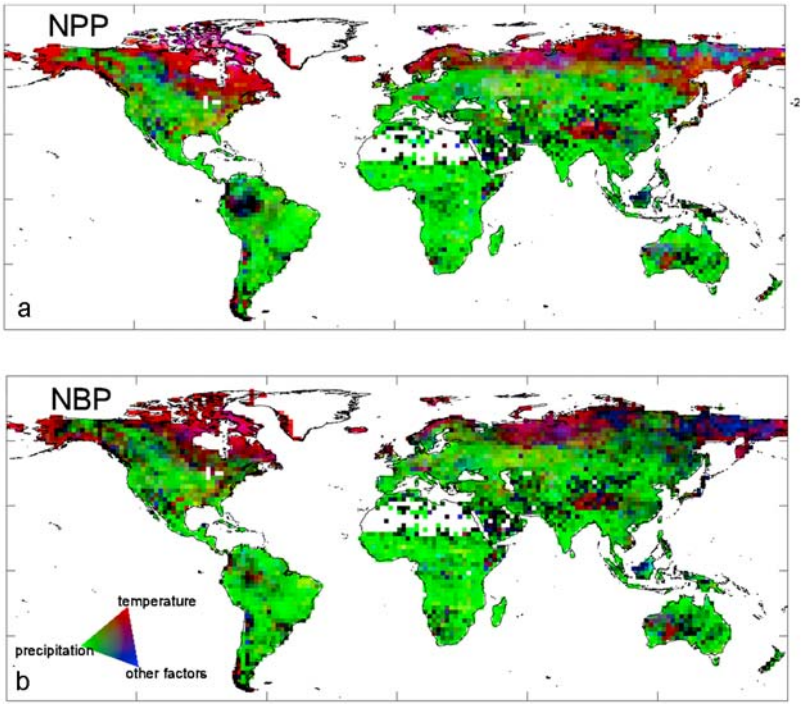

Figure 8. Spatial distribution of climatic controls on interannual variation of NPP and NBP due to temperature, precipitation, and other climate factors. Red color indicates that the interannual variation of modeled C flux is primarily explained by temperature change, green color indicates that the interannual variation of modeled C flux is primarily explained by precipitation change, and blue color indicates that other climate factors (e.g., solar radiation and humidity) play a dominant role.

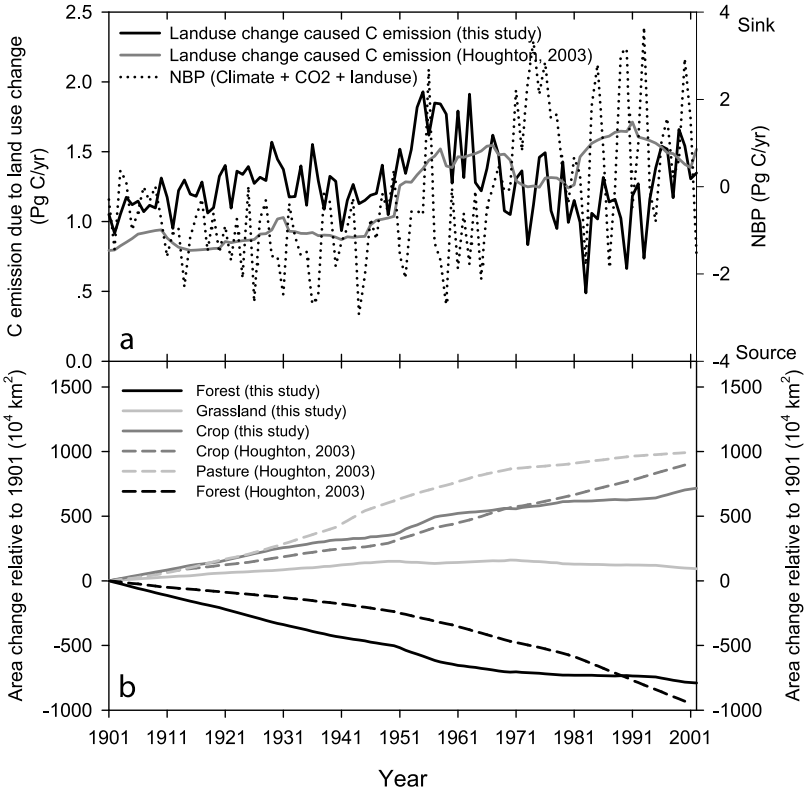

Figure 9. Change in carbon emissions from land use change (simulation S6 – S5), net carbon exchange (NBP) associated with all factors including climate, atmospheric CO_2 and land use (simulation S1 + S6 – S5), and crop land area from 1901 to 2002.

change is still more strongly associated with the interannual variation in NBP than other climatic factors, particularly in temperate and tropical regions, further supporting the conclusion that precipitation change is primarily driver of the global NBP variability [*Schaefer et al.*, 2002; *Zeng et al.*, 2005].

5. Effects of Land Use Change on C Balance

[30] In this section, we analyze the effects of land use change on terrestrial C balance over the last century. As mentioned in section 1, we performed two new simulations (simulation S5 and S6) without considering natural fire disturbances (see discussion in section 6.3). In simulation S5, only atmospheric CO_2 and climate were varied over the last century, while in simulation S6 atmospheric CO_2 and climate as well as land use were varied. The individual effect of land use changes were estimated by subtracting S5 from the S6 results. Similar to simulation S1, both simulations are initialized in 1860 with repeated climate conditions from the 1901–1910 period, the 1860 atmospheric CO_2 concentration of 286.05 ppm, and 1860 land cover.

5.1. Global Scale

[31] The global NBP changes associated with land use change over the last century is shown in Figure 9. The land use change caused global C emission showed increasing trend until 1950s, and then sharply decreased during the period 1960–1990 (Figure 9a), which is consistent with the change in area of cropland (Figure 9b). Furthermore, it was converted to slightly increase since 1990. Such variation in land use change caused a mean CO_2 source to the atmosphere. However, it is not strong enough to affect the modeled interannual variation in net C exchange between terrestrial ecosystem and atmosphere ($R^2 = 0.04$, between S6 – S5 and S1), reflecting the dominant role of climate in the interannual variation of net C exchange ($R^2 = 0.97$).

[32] Over the last century, the modeled land use change emitted about 129 Pg of C to the atmosphere. About 76% (or 98 Pg C) of this emission, however, was offset by the net C uptake on land driven by changes in climate and CO_2 (simulation S1) in other regions. Thus, the modeled net release of C from the terrestrial ecosystems to the atmosphere from 1901 to 2002 is about 31 Pg C, reflecting that 20% of the increase in atmospheric CO_2 concentration was contributed by the feedback of terrestrial C cycle to the atmosphere over the last century. For the period 1980s and 1990s, climate change and CO_2 rising (simulation S1) forced C uptake (1.6 Pg C yr^{-1} for 1980s and 2.2 Pg C yr^{-1} for 1990s) is much larger than land use change driven C emission (1.0 Pg C yr^{-1} for 1980s and 1.2 Pg C yr^{-1} for 1990s), leading to a net C sink of 0.5 Pg C yr^{-1} in 1980s and of 1.0 Pg C yr^{-1} in the 1990s (Figure 9a).

5.2. Spatial Patterns

[33] In response to land use change over the last century, the largest C emission (>10 gC m^{-2} yr^{-1}) is mainly distributed in central North America, eastern Europe, South

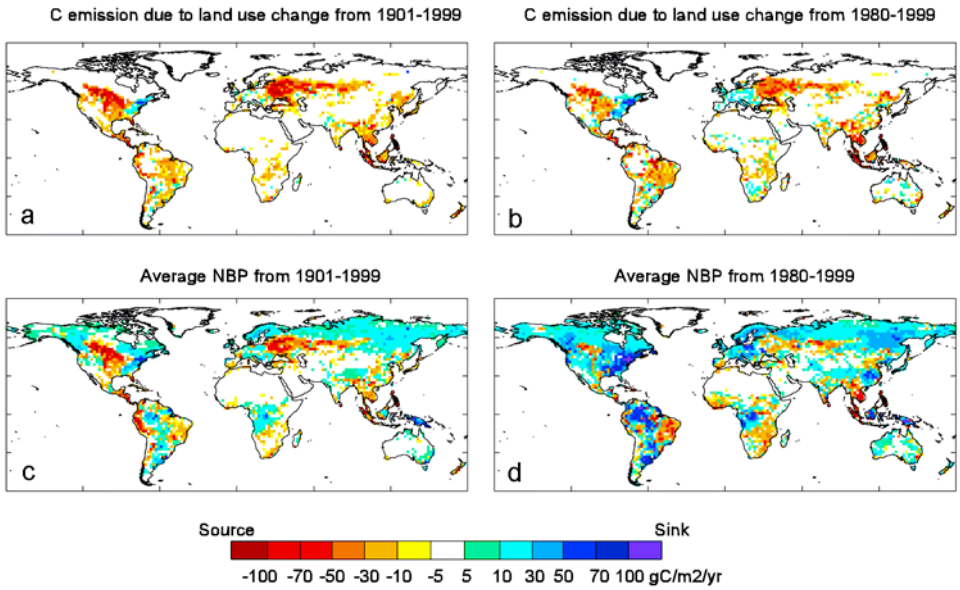

Figure 10. Spatial distribution of carbon emissions from land use change (simulation S6 − S5) and net carbon exchange (NBP) associated with all factors including climate, atmospheric CO_2 and land use (simulation S1 + S6 − S5) for the periods 1901–1999 and 1980–1999.

Asia and eastern South America (Figure 10a). Only a few areas principally in North America and Europe exhibit a considerable decrease of crop area during the last century. Consequently, net C uptake is detected as a legacy of past land use changes across these regions (Figure 10a). In comparison to the period 1901–1999, land use change caused C emission in central North America and eastern Europe is somewhat decreased (Figure 10b). In contrast, C emission in tropical regions is slightly increased (Table 2). Due to forest regrowth, central Europe has a net C uptake associated with land use change during 1980–1999 (Figure 10b). We estimate that the net C uptake from European land use change in the 1980s and 1990s is about 0.01 PgC yr^{-1} and 0.02 PgC yr^{-1}, respectively (Table 2).

[34] Figures 10c and 10d show the spatial distribution of NBP associated with climate, CO_2, and land use change (S1 + S6 − S5) for the periods 1901–1999 and 1980–1999, respectively. Due to strong land use change caused C emission which largely offsets the climate and CO_2 induced sinks, a net C source is obtained in the North American middle west agricultural regions) and in eastern Europe over the last century (Figure 10c). Both regions experienced a strong expansion of croplands over natural grasslands and forests, and the ''carbon debt'' of these early century changes in land use has not yet been recovered. Eastern South America and southwestern Africa also show net land use induced C emission during the period 1901–1999. Similar spatial patterns of NBP is observed during 1980–1999 (Figure 10d), but the net C uptake in most of temperate and

Table 2. Carbon Emissions From Land Use Change (Simulation S6 − S5) and Net Carbon Exchange Associated With All Factors[a]

	Carbon Emission due to Land Use Change (Pg C yr^{-1})								NBP (Pg C yr^{-1})		
	This Study (Simulation S6 − S5)			*Houghton* [2003]		*Jain and Yang* [2005]	Other Studies		This Study (Simulation S1 + S6 − S5)		
Region	1901–1999	1980s	1990s	1980s	1990s	1980s	1980s	1990s	1901–1999	1980s	1990s
Tropical America	0.27	0.28	0.38	0.77	0.75	0.24	0.4[b]	0.5[b]	−0.12	0.24	0.00
Tropical Africa	0.07	0.07	0.12	0.28	0.35	0.08	0.1[b]	0.1[b]	−0.01	−0.21	0.05
Tropical Asia	0.19	0.27	0.25	0.88	1.09	0.34	0.2[b]	0.4[b]	−0.07	−0.15	−0.08
Tropics	0.54	0.62	0.74	1.93	2.20	0.67	0.7[b]	1.0[b]	−0.20	−0.13	−0.03
North America	0.23	0.12	0.07	−0.09	−0.08	0.01			−0.08	0.24	0.53
Europe	0.03	−0.01	−0.02	−0.02	−0.02	0.00			0.02	0.10	0.09
Former Soviet Union	0.29	0.20	0.23	0.03	0.02	0.00			−0.02	0.16	0.29
China	0.07	0.03	0.13	0.11	0.03	−0.03			−0.02	0.13	0.02
Global	1.27	1.03	1.22	1.99	2.18	0.67	0.6–1.0[c]		−0.31	0.55	0.99

[a]Factors include climate, atmospheric CO_2, and land use (simulation S1 + S6 − S5). Positive values of net carbon exchange (NBP) represent net carbon uptake.
[b]*DeFries et al.* [2002].
[c]*Mcguire et al.* [2001].

boreal regions is higher than the average value of last century due to the effects of climate change and rising atmospheric CO_2.

6. Discussion

6.1. NPP Changes

[35] Previous observational and modeling studies have documented that terrestrial photosynthetic activity has increased over the past 2–3 decades [*Fang et al.*, 2003; *Nemani et al.*, 2003; *Boisvenue and Running*, 2006]. Using a satellite-based model of NPP, *Nemani et al.* [2003] inferred that global NPP increased by 0.34% yr^{-1} over the past 2 decades, which is close to our modeling result (0.4% yr^{-1}).

[36] There has been much debate about the cause of such a significant increase in NPP. Although satellite-based models could relatively accurately estimate the change in vegetation NPP, it is still a great challenge using these models to understand the mechanisms because remotely sensed greenness observations result from the combined effects of several factors, such as climate change, rising atmospheric CO_2 concentration, nitrogen deposition and land management [*Nemani et al.*, 2003]. Process models that describe major biogeochemical behaviors influencing the C processes are potentially effective tools for this purpose. Previous modeling experiments showed that rising atmospheric CO_2 concentration is primarily responsible for the current increase in global NPP [*Friedlingstein et al.*, 1995; *Friend et al.*, 2007], although there also remain large uncertainties in attempts to model the direct effects of CO_2 fertilization on plant growth [*Bazzaz et al.*, 1995]. Recently, *Norby et al.* [2005] analyzed the response of NPP to elevated CO_2 in four free-air CO_2 enrichment (FACE) experiments in forest stands and showed that the enhancement of forest NPP by rising CO_2 (about 180 ppmv) is about 23%. Assuming a linear extrapolation from these FACE site results, the increased atmospheric CO_2 concentration from 338 ppmv in 1980 to 378 ppmv in 2002 would imply approximately a 5% increase in global NPP during the study period, which is consistent with our modeling result. In response solely to atmospheric CO_2 change (simulation S2), the modeled global NPP increased by about 6%, accounting for 80% of the increase in simulation S1.

[37] Recent climate change alone also leads to increase in global NPP, but its relative contribution is not constant across global land surface. Some studies have showed a strong link between enhanced vegetation growth and warming in the northern region [*Zhou et al.*, 2001]. This is consistent with our simulation result that annual NPP in boreal region increased with current rising temperature (see Figure 8). Global warming might be expected to have strong negative impacts on vegetation growth in already warm regions, by increasing the potential evapotranspiration. Indeed, our simulations reveal that, unlike in boreal ecosystems, the current rise in temperature alone does not benefit to vegetation NPP in temperate and tropical ecosystems (water-controlled biomes in Figure 8), a response probably associated with reduced soil moisture content. Such a negative relationship between temperature and tree growth is also observed in historical tree ring record for both tropical forest and temperate forest [*Clark et al.*, 2003; *Liang et al.*, 2003], suggesting that water availability is a key limiting factor controlling vegetation NPP in these regions. This is further evident from the 2003 summer drought in Europe [*Ciais et al.*, 2005] and the recent dry summers in mid and high northern latitudes [*Angert et al.*, 2005]. Current precipitation change is an important factor responsible for enhanced vegetation productivity in the Southern Hemisphere (south of 20°S) and tropical region, where precipitation change alone has led to significant increase in annual NPP by about 0.26% yr^{-1} and 0.15% yr^{-1}, respectively, contributing about 40% of the annual NPP increase. In addition, our results suggest that in response to land use changes (S6 – S5), global NPP has not significantly increased over the last 2 decades ($R^2 = 0.04$, $P < 0.10$), implying that the contribution of land use change to the increasing trend of global NPP over the last 2 decades may be limited.

6.2. NBP Associated With the Change in Climate and CO_2

[38] Figure 11 shows the comparison of interannual variation in our modeled global NBP with the anomalous flux deduced from one atmospheric inversion and from the LPJ bottom-up model (same data as given by *Peylin et al.*, 2005). Generally, the representation of interannual timing and magnitude of NBP variations in the ORCHIDEE is better during 1990s than during 1980s. For example, ORCHIDEE produces a negative anomaly of NBP in 1998 (an El Niño year) which is very close to that derived from inverse modeling, while both ORCHIDEE and LPJ estimated anomaly of NBP in 1983 (another El Niño year) is somewhat stronger than that from inverse modeling. This is probably due to the limited number of atmospheric stations (less than 25) before 1985 [*Peylin et al.*, 2005]. One can also note that after the cooling induced by aerosols emitted by the volcanic eruption of Mount Pinatubo in June 1991, the global NBP increased during the period 1992–1993, but the increasing magnitude from ORCHIDEE (and LPJ as well) is larger than that analyzed by the inversion.

[39] In addition to interannual variability, the magnitude of current global NBP without considering land use change is generally comparable to earlier estimates. We estimated that global annual NBP in the 1980s attributed to climate change and CO_2 fertilization is about 1.6 Pg C yr^{-1}, which is within the range of 1.1–2.3 Pg C yr^{-1} derived from other terrestrial models [*McGuire et al.*, 2001; *Jain and Yang*, 2005]. About 70% of our estimated land C sink is distributed in the Northern Hemisphere, consistent with the result detected by atmospheric inversion modeling [*Ciais et al.*, 1995; *IPCC*, 2007].

[40] Climate change and CO_2 fertilization caused global land C sink in the 1990s is larger by about 0.6 Pg C yr^{-1} than that in the 1980s. Such increase in global NBP is mainly distributed in boreal and tropical regions, contributing about 70% of the increasing NBP over the last 2 decades. Our results also show that rising atmospheric CO_2 made a greater contribution to the increased global NBP (simulation S1) than climate change. It is noteworthy that although both

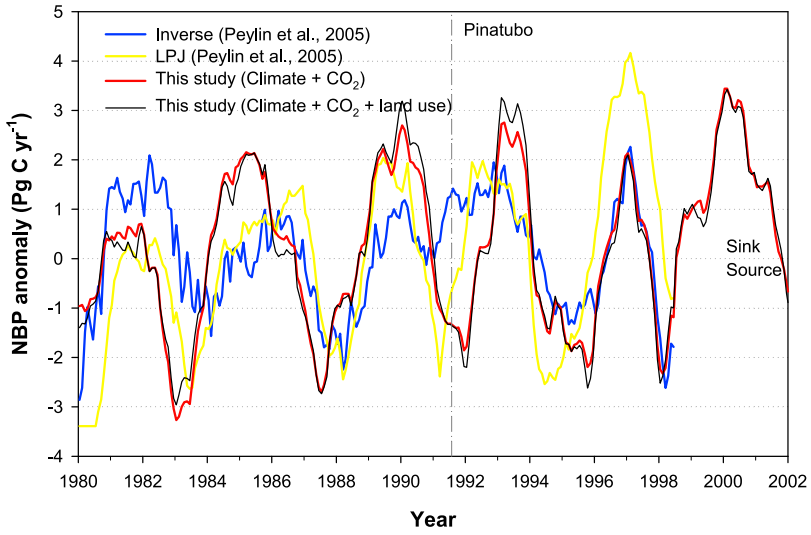

Figure 11. Anomalies in NBP obtained from this study, LPJ model, and atmospheric inverse model [*Peylin et al.*, 2005] over the past 2 decades. Positive values represent carbon uptake, and negative values represent carbon release.

this study and several previous analyses [*Lucht et al.*, 2002; *Piao et al.*, 2006] highlighted a significantly enhanced vegetation productivity in response to recent warming in boreal ecosystems, a small, warming-induced, decreasing trend was present for the modeled annual NBP at the continental scale ($R = 0.20$, $P > 0.05$). This result indicates that rising temperature will not necessarily increase net C uptake in high-latitude regions owing to concurrent stimulation of HR which is normally more sensitive to temperature change than NPP [*Vukicevic et al.*, 2001; *Cao et al.*, 2002].

6.3. NBP Associated With Land Use Change

[41] Current lack of information on the amount and spatial patterns of deforestation and impacted forest biomass stock [*Houghton*, 2007] makes it extremely challenging to accurately estimate the magnitude of NBP changes associated with land use change, particularly in tropical region [*DeFries et al.*, 2002]. Although our modeled total C emission (129 Pg C) from land use change during the last century is comparable with the previous estimation of 120 Pg C derived by bookkeeping model [*Houghton*, 2003], there is a large difference in its temporal and spatial patterns due to different rate of temporal change in cropland area (Table 2 and Figure 9). During the period 1901–1960, the ORCHIDEE modeled results produce generally a larger source than those of *Houghton* [2003], although both estimations show increasing trends in global C emission driven by land use change. Since about 1960, the net source due to tropical forest clearing estimated by *Houghton* [2003] exceeded our estimate, particularly during the 1980s.

[42] At the global scale, our inferred land use flux to the atmosphere (1.0 Pg C yr^{-1} for 1980s and 1.2 Pg C yr^{-1} for 1990s) is only 50% of the one derived from the book keeping model of *Houghton* [2003] (1.99 Pg C yr^{-1} for 1980s and 2.18 Pg C yr^{-1} for 1990s). This discrepancy mainly arises from the very different prescribed rates of cropland area changes (Figure 9). The study of *Jain and Yang* [2005] suggested that the land use source in the 1980s was nearly doubled when applying the cropland area of *Houghton* [2003] instead of the one of *Ramankutty and Foley* [1999], but their estimation (0.6–1.3 Pg C yr^{-1}) was still not as large as estimated by *Houghton* [2003]. Our calculated land use flux of 1.0 Pg C yr^{-1}, is considerably larger than that of *Jain and Yang* [2005] (0.67 Pg yr^{-1}), and larger than that of *McGuire et al.* [2001], although all three carbon models were prescribed the same *Ramankutty and Foley* [1999] cropland data set. Such larger C emission in response to land use change may be caused by our set up and different simulation scenarios (Table 1). Because most deforestation has occurred in moist tropical forests with a very long natural fire return interval, we calculated the effect of forest clearing on C balance without considering natural fire disturbances. To check on this indirect effect of fires on the land use flux, we also integrated ORCHIDEE by activating natural fire disturbances. The results indicate that in comparison with the simulation results without fire disturbance, annually about 0.3 Pg (or 30%) of less C emission from land use change is estimated when fires are included (Figure 12). This finding illustrates the indirect importance of natural fires in the calculation of C emissions associated with land use change.

[43] The largest difference in land use flux between our new estimation and *Houghton* [2003] lies in tropical regions. The ORCHIDEE simulated land use flux is of 0.62 Pg C yr^{-1} in 1980s and 0.74 Pg C yr^{-1} in 1990s, which is only 30% of the source given by *Houghton* [2003] (1.9 Pg C yr^{-1} in 1980s and 2.2 Pg C yr^{-1} in 1990s). An assessment based on satellite data and the latest published information on forest biomass, however, also challenges the estimation by *Houghton* [2003] as unrealistically high, claiming that the deforestation induced source of C was about 0.7 Pg C yr^{-1} in 1980s and 1.0 Pg C yr^{-1} in 1990s [*DeFries et al.*, 2002], still slightly larger than our numbers (Table 2). As stated above, uncertainties associated with the

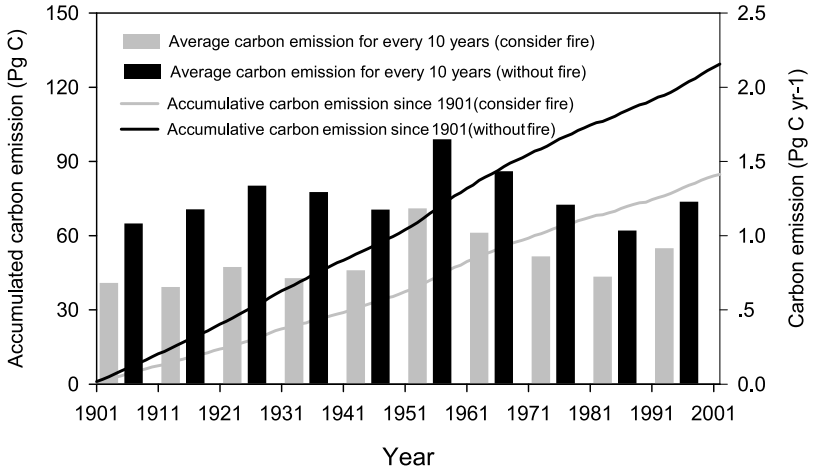

Figure 12. Comparison of modeled carbon emissions from land use change between fire simulation and fire-excluded simulation.

historical rate of change in croplands and in pasture area (Figure 9) contribute largely to the spread of estimates. Due to the smaller C emission associated with land use change, our modeling results suggest the net carbon balance of tropical lands is close to neutral (about 0.13 Pg C yr^{-1} in 1980s and 0.03 Pg C yr^{-1} in 1990s). This result is comparable to the terrestrial carbon model analysis of *Jain and Yang* [2005], but it does not support inverse modeling estimation derived from atmospheric inversions models (1.2 ± 1.2 Pg C yr^{-1}) [*Gurney et al.*, 2002]. The recent cross validation study of *Stephens et al.* [2007] using vertical CO_2 profiles revealed a common bias of nearly all of these transport models, with the few models which closely reproduced the vertical CO_2 profiles giving a weaker net tropical emission of 0.1 PgC yr^{-1}.

6.4. Limitation and Next Steps

[44] Several uncertainties are existed in our current simulation due to the uncertainty of model input such as climate forcing data and historical land use information. For example, due to the lack of historical climate data with high temporal resolution (e.g., half-hourly time step), the monthly CRU climate data were interpolated to half-hourly weather variables using a weather generator, which may be one of the big sources of uncertainty in our simulation. Regarding historical land use changes, we only include the effects of deforestation during the agricultural conversion to croplands and pastures as well as agricultural abandonment, while the effects of wood harvesting and forest regrowth are not included in our study, although they may play a significant role in shaping historic C fluxes, especially in North America and Eurasia. This may be one of the causes for the overestimates of land use change driven C emission for Northern Hemisphere in the 1980s and 1990s, particularly in North America (0.10 Pg C yr^{-1} of this study versus −0.09 Pg C yr^{-1} of *Houghton* [2003]). In addition, the effects of no-tillage management practice on the C balance are also not taken into account in this study. To quantify and reduce uncertainties of C balance caused by these model input data set, spatially and temporally explicit historic climate and land cover/use data sets are needed.

[45] It should be noted that the ORCHIDEE model still misses some processes, which could lead to some misinterpretation. First, our simulation did not consider the effects of nitrogen limitation and of nitrogen deposition on the C cycle. Ignoring nitrogen limitations may yield to overestimate the CO_2 fertilization effect on vegetation growth in the model. N deposition is generally expected to enhance the net C sink across temperate and boreal forests, but the magnitude of its contribution is still poorly quantified due to our current lack of knowledge on the N cycle process [*Magnani et al.*, 2007; *Churkina et al.*, 2007; *Sutton et al.*, 2008]. Second, the effects of ozone pollution are also not taken into account for this study. It was found that increase in the tropospheric ozone level will decline vegetation growth [*Adams et al.*, 1989; *Sitch et al.*, 2007]. Thus, the increase in NPP may have been overestimated in our study, given greater rates of ozone pollution over the last 2 decades. However, it is possible that the negative effects of ozone pollution are compensated by enhanced vegetation growth due to N deposition. Finally, human managements including fertilization and irrigation may also substantially influence C cycle at regional scales [*Bondeau et al.*, 2007; *Gervois et al.*, 2008], but it is not considered in this study. The effects of cultivation on crop soil C decomposition rate are simply parameterized by multiplying a cultivation factor (1.3 for C4 crops and 1.1 for C3 crops), while pastureland is simply treated as nature grassland, since we currently know far too little about the C cycle processes for crop and pastureland as well as their response to human disturbance. Further studies are needed to quantify the effects of all these factors on global terrestrial C balance.

7. Conclusions

[46] The results of this study, which attempts to use a recently developed ecosystem model to calculate the historical changes in regional C fluxes, show complex responses of regional C balance to changes in climate, atmospheric CO_2, and land use. The global C cycle has been accelerated under current climate change and rising atmospheric CO_2 concentration, which led to enhanced vegetation productivity

and a faster turnover of the terrestrial C reservoirs. While global terrestrial ecosystems act as a small C sink and its magnitude tends to increase slightly over the last 2 decades, our calculations also suggest that current global warming has already begun to accelerate C loss in tropical and temperate regions, offsetting about 70% of the increase in global NBP due to CO_2 fertilization effects. We expect such a response will act as a positive feedback to global warming in the coming decades [*Cox et al.*, 2000; *Friedlingstein et al.*, 2006]. Further, land use change dramatically affects current C balance, although our estimation of the land use flux is only half of a previous estimation by *Houghton* [2003]. Accordingly, our results suggest that net carbon balance of tropical lands is close to neutral over the past 2 decades, supporting current inversion analysis by *Stephens et al.* [2007]. To help resolve this discrepancy and to more accurately quantify the effects of land use change on the C balance, it is desirable to develop reliable historical global land use map with high spatial and temporal resolution.

References

Adams, R. M., J. D. Glyer, S. L. Johnson, and B. A. McCarl (1989), A reassessment of the economic effects of ozone on U.S. agriculture, *JAPCA*, *39*, 960–968.

Angert, A., S. Biraud, C. Bonfils, C. C. Henning, W. Buermann, J. Pinzon, C. J. Tucker, and I. Fung (2005), Drier summers cancel out the CO_2 uptake enhancement induced by warmer springs, *Proc. Natl. Acad. Sci. U. S. A.*, *102*, 10,823–10,827, doi:10.1073/pnas.0501647102.

Arrouays, D., et al. (Eds.) (2002), Increasing carbon stocks in French agricultural soils? Synthesis of an assessment report by the French Institute for Agricultural Research on request of the French Ministry for Ecology and Sustainable Development, Sci. Assess. Unit for Expertise, INRA, Paris.

Bazzaz, F. A., M. Jasienski, S. C. Thomas, and P. Wayne (1995), Microevolutionary responses in experimental populations of plants to CO_2-enriched environments: Parallel results from two model systems, *Proc. Natl. Acad. Sci. U. S. A.*, *92*, 8161–8165, doi:10.1073/pnas.92.18.8161.

Behrenfeld, M. J., et al. (2001), Biospheric primary production during an ENSO transition, *Science*, *291*, 2594–2597, doi:10.1126/science.1055071.

Boisvenue, C., and S. W. Running (2006), Impacts of climate change on natural forest productivity: Evidence since the middle of the 20th century, *Global Change Biol.*, *12*, 862–882, doi:10.1111/j.1365-2486.2006.01134.x.

Bondeau, A., et al. (2007), Modelling the role of agriculture for the 20th century global terrestrial carbon balance, *Global Change Biol.*, *13*, 679–706, doi:10.1111/j.1365-2486.2006.01305.x.

Buyanovsky, G. A., and G. H. Wagner (1998), Carbon cycling in cultivated land and its global significance, *Global Change Biol.*, *4*, 131–141, doi:10.1046/j.1365-2486.1998.00130.x.

Campbell, G. S., and J. M. Norman (1998), *An Introduction to Environmental Biophysics*, Springer, New York.

Cao, M. K., S. D. Prince, and H. H. Shugart (2002), Increasing terrestrial carbon uptake from the 1980s to the 1990s with changes in climate and atmospheric CO_2, *Global Biogeochem. Cycles*, *16*(4), 1069, doi:10.1029/2001GB001553.

Churkina, G., and S. W. Running (1998), Contrasting climatic controls on the estimated productivity of global terrestrial biomes, *Ecosystems*, *1*, 206–215, doi:10.1007/s100219900016.

Churkina, G., K. Trusilova, M. Vetter, and F. Dentener (2007), Contributions of nitrogen deposition and forest regrowth to terrestrial carbon uptake, *Carbon Balance Manage.*, *2*, 5, pp., doi:10.1186/1750-0680-2-5.

Ciais, P., P. P. Tans, M. Trolier, and R. J. Francey (1995), A large Northern Hemisphere terrestrial CO_2 sink indicated by the $^{13}C/^{12}C$ ratio of atmospheric CO_2, *Science*, *269*, 1098–1102, doi:10.1126/science.269.5227.1098.

Ciais, P., et al. (2005), Europe-wide reduction in primary productivity caused by the heat and drought in 2003, *Nature*, *437*, 529–533, doi:10.1038/nature03972.

Clark, D. A., S. C. Piper, C. D. Keeling, and D. B. Clark (2003), Tropical rain forest tree growth and atmospheric carbon dynamics linked to interannual temperature variation during 1984–2000, *Proc. Natl. Acad. Sci. U. S. A.*, *100*, 5852–5857, doi:10.1073/pnas.0935903100.

Collatz, G. J., M. Ribas-Carbo, and J. A. Berry (1992), Coupled photosynthesis-stomatal conductance model for leaves of C4 plants, *Aust. J. Plant Physiol.*, *19*, 519–538.

Cox, P. M., R. A. Betts, C. D. Jones, S. A. Spall, and I. J. Totterdell (2000), Acceleration of global warming due to carbon-cycle feedbacks in a coupled climate model, *Nature*, *408*, 184–187, doi:10.1038/35041539.

Davidson, E. A., and I. A. Janssens (2006), Temperature sensitivity of soil carbon decomposition and feedbacks to climate change, *Nature*, *440*, 165–173, doi:10.1038/nature04514.

DeFries, R. S., R. A. Houghton, M. C. Hansen, C. B. Field, D. Skole, and J. Townshend (2002), Carbon emissions from tropical deforestation and regrowth based on satellite observations for the 1980s and 1990s, *Proc. Natl. Acad. Sci. U. S. A.*, *99*, 14,256–14,261, doi:10.1073/pnas.182560099.

Erbrecht, T., and W. G. Lucht (2006), Impacts of large-scale climatic disturbances on the terrestrial carbon cycle, *Carbon Balance Manage.*, *1*, 7, pp., doi:10.1186/1750-0680-1-7.

Fang, J. Y., S. L. Piao, C. B. Field, Y. Pan, Q. H. Guo, L. M. Zhou, C. H. Peng, and S. Tao (2003), Increasing net primary production in China from 1982 to 1999, *Front. Ecol. Environ*, *1*, 293–297.

Fang, J. Y., S. L. Piao, L. M. Zhou, J. S. He, F. Y. Wei, R. B. Myneni, C. J. Tucker, and K. Tan (2005), Precipitation patterns alter growth of temperate vegetation, *Geophys. Res. Lett.*, *32*, L21411, doi:10.1029/2005GL024231.

Farquhar, G. D., S. V. Caemmerer, and J. A. Berry (1980), A biochemical-model of photosynthetic CO_2 assimilation in leaves of C_3 species, *Planta*, *149*, 78–90, doi:10.1007/BF00386231.

Friedlingstein, P., I. Fung, E. Holland, J. John, G. Brasseur, D. Erickson, and D. Schimel (1995), On the contribution of CO_2 fertilization to the missing biospheric sink, *Global Biogeochem. Cycles*, *9*, 541–556, doi:10.1029/95GB02381.

Friedlingstein, P., G. Joel, C. B. Field, and I. Y. Fung (1999), Toward an allocation scheme for global terrestrial carbon models, *Global Change Biol.*, *5*, 755–770, doi:10.1046/j.1365-2486.1999.00269.x.

Friedlingstein, P., et al. (2006), Climate-carbon cycle feedback analysis: Results from the (CMIP)-M-4 model intercomparison, *J. Clim.*, *19*, 3337–3353, doi:10.1175/JCLI3800.1.

Friend, A. D. (1998), Parameterization of a global daily weather generator for terrestrial ecosystem modelling, *Ecol. Modell.*, *109*, 121–140, doi:10.1016/S0304-3800(98)00036-2.

Friend, A. D., et al. (2007), FLUXNET and modelling the global carbon cycle, *Global Change Biol.*, *13*, 610–633, doi:10.1111/j.1365-2486.2006.01223.x.

Gervois, S., P. Ciais, N. de Noblet-Ducoudre, N. Brisson, and N. Vuichard (2008), Carbon and water balance of European croplands throughout the 20th century, *Global Biogeochem. Cycles*, *22*, GB2022, doi:10.1029/2007GB003018.

Gitz, V., and P. Ciais (2003), Amplifying effects of land-use change on future atmospheric CO_2 levels, *Global Biogeochem. Cycles*, *17*(1), 1024, doi:10.1029/2002GB001963.

Goldewijk, K. K. (2001), Estimating global land use change over the past 300 years: The HYDE database, *Global Biogeochem. Cycles*, *15*, 417–433, doi:10.1029/1999GB001232.

Gurney, K. R., et al. (2002), Towards robust regional estimates of CO_2 sources and sinks using atmospheric transport models, *Nature*, *415*, 626–630, doi:10.1038/415626a.

Hashimoto, H., R. R. Nemani, M. A. White, W. M. Jolly, S. C. Piper, C. D. Keeling, R. B. Myneni, and S. W. Running (2004), El Niño–Southern Oscillation–induced variability in terrestrial carbon cycling, *J. Geophys. Res.*, *109*, D23110, doi:10.1029/2004JD004959.

Hicke, J. A., and D. B. Lobell (2004), Spatiotemporal patterns of cropland area and net primary production in the central United States estimated from USDA agricultural information, *Geophys. Res. Lett.*, *31*, L20502, doi:10.1029/2004GL020927.

Houghton, R. A. (2000), Interannual variability in the global carbon cycle, *J. Geophys. Res.*, *105*, 20,121–20,130, doi:10.1029/2000JD900041.

Houghton, R. A. (2003), Revised estimates of the annual net flux of carbon to the atmosphere from changes in land use and land management 1850–2000, *Tellus, Ser. B*, *55*, 378–390, doi:10.1034/j.1600-0889.2003.01450.x.

Houghton, R. A. (2007), Balancing the global carbon budget, *Annu. Rev. Earth Planet. Sci.*, *35*, 313–347, doi:10.1146/annurev.earth.35.031306.140057.

IPCC (2007), *Climate Change 2007. The Physical Science Basis: Summary for Policymakers*, Intergov. Panel on Clim. Change Secretariat, Geneva.

Jain, A. K., and X. J. Yang (2005), Modeling the effects of two different land cover change data sets on the carbon stocks of plants and soils in

concert with CO2 and climate change, *Global Biogeochem. Cycles*, *19*, GB2015, doi:10.1029/2004GB002349.

Jones, C. D., M. Collins, P. M. Cox, and S. A. Spall (2001), The carbon cycle response to ENSO: A coupled climate-carbon cycle model study, *J. Clim.*, *14*, 4113–4129, doi:10.1175/1520-0442(2001)014<4113:TCCRTE>2.0.CO;2.

Keeling, C. D., T. P. Whorf, M. Wahlen, and J. Vanderplicht (1995), Interannual extremes in the rate of rise of atmospheric carbon-dioxide since 1980, *Nature*, *375*, 666–670, doi:10.1038/375666a0.

Kirschbaum, M. U. F. (2000), Will changes in soil organic carbon act as a positive or negative feedback on global warming?, *Biogeochemistry*, *48*, 21–51, doi:10.1023/A:1006238902976.

Krinner, G., et al. (2005), A dynamic global vegetation model for studies of the coupled atmosphere-biosphere system, *Global Biogeochem. Cycles*, *19*, GB1015, doi:10.1029/2003GB002199.

Law, R. M., E. A. Kowalczyk, and Y. P. Wang (2006), Using atmospheric CO_2 data to assess a simplified carbon-climate simulation for the 20th century, *Tellus, Ser. B*, *58*, 427–437, doi:10.1111/j.1600-0889.2006.00198.x.

Liang, E. Y., X. M. Shao, Z. C. Kong, and J. X. Lin (2003), The extreme drought in the 1920s and its effect on tree growth deduced from tree ring analysis: A case study in north China, *Ann. For. Sci.*, *60*, 145–152, doi:10.1051/forest:2003007.

Loveland, T. R., B. C. Reed, J. F. Brown, D. O. Ohlen, Z. Zhu, L. Yang, and J. W. Merchant (2000), Development of a global land cover characteristics database and IGBP DISCover from 1 km AVHRR data, *Int. J. Remote Sens.*, *21*, 1303–1330, doi:10.1080/014311600210191.

Lucht, W., I. C. Prentice, R. B. Myneni, S. Sitch, P. Friedlingstein, W. Cramer, P. Bousquet, W. Buermann, and B. Smith (2002), Climatic control of the high-latitude vegetation greening trend and Pinatubo effect, *Science*, *296*, 1687–1689, doi:10.1126/science.1071828.

Magnani, F., et al. (2007), The human footprint in the carbon cycle of temperate and boreal forests, *Nature*, *447*, 848–850, doi:10.1038/nature05847.

McGuire, A. D., et al. (2001), Carbon balance of the terrestrial biosphere in the twentieth century: Analyses of CO_2, climate and land use effects with four process-based ecosystem models, *Global Biogeochem. Cycles*, *15*, 183–206, doi:10.1029/2000GB001298.

McNaughton, S. J., M. Oesterheld, D. A. Frank, and K. J. Williams (1989), Ecosystem-level patterns of primary productivity and herbivory in terrestrial habitats, *Nature*, *341*, 142–144, doi:10.1038/341142a0.

Mitchell, T. D., and P. D. Jones (2005), An improved method of constructing a database of monthly climate observations and associated high-resolution grids, *Int. J. Climatol.*, *25*, 693–712, doi:10.1002/joc.1181.

Murty, D., M. U. F. Kirschbaum, R. E. McMurtrie, and A. McGilvray (2002), Does conversion of forest to agricultural land change soil carbon and nitrogen? A review of the literature, *Global Change Biol.*, *8*, 105–123, doi:10.1046/j.1354-1013.2001.00459.x.

Nemani, R. R., C. D. Keeling, H. Hashimoto, W. M. Jolly, S. C. Piper, C. J. Tucker, R. B. Myneni, and S. W. Running (2003), Climate-driven increases in global terrestrial net primary production from 1982 to 1999, *Science*, *300*, 1560–1563, doi:10.1126/science.1082750.

Nicks, A. D., C. W. Richardson, and J. R. Williams (1990), Evaluation of the EPIC model weather generator, in *Erosion/Productivity Impact Calculator, 1. Model Documentation*, *USDA-ARS Tech. Bull.*, *1768*(235), edited by A. N. Sharpley and J. R. Williams, pp. 105–124, Govt. Print. Off., Washington, D. C.

Norby, R. J., et al. (2005), Forest response to elevated CO2 is conserved across a broad range of productivity, *Proc. Natl. Acad. Sci. U. S. A.*, *102*, 18,052–18,056, doi:10.1073/pnas.0509478102.

Parton, W. J., J. W. B. Stewart, and C. V. Cole (1988), Dynamics of C, N, P and S in grassland soils: A model, *Biogeochemistry*, *5*, 109–131, doi:10.1007/BF02180320.

Peylin, P., P. Bousquet, C. LeQuere, S. Sitch, P. Friedlignstein, G. Mckinley, N. Gruber, P. Rayner, and P. Ciais (2005), Multiple constraints on regional CO_2 flux variations over land and oceans, *Global Biogeochem. Cycles*, *19*, GB1011, doi:10.1029/2003GB002214.

Piao, S. L., P. Friedlingstein, P. Ciais, L. M. Zhou, and A. P. Chen (2006), Effect of climate and CO2 changes on the greening of the Northern Hemisphere over the past two decades, *Geophys. Res. Lett.*, *33*, L23402, doi:10.1029/2006GL028205.

Piao, S. L., et al. (2008), Net carbon dioxide losses of northern ecosystems in response to autumn warming, *Nature*, *451*, 49–52, doi:10.1038/nature06444.

Ramankutty, N., and J. A. Foley (1999), Estimating historical changes in global land cover: Croplands from 1700 to 1992, *Global Biogeochem. Cycles*, *13*, 997–1027, doi:10.1029/1999GB900046.

Reichstein, M., et al. (2007), Determinants of terrestrial ecosystem carbon balance inferred from European eddy covariance flux sites, *Geophys. Res. Lett.*, *34*, L01402, doi:10.1029/2006GL027880.

Richardson, C. W. (1981), Stochastic simulation of daily precipitation, temperature, and solar radiation, *Water Resour. Res.*, *17*, 182–190, doi:10.1029/WR017i001p00182.

Richardson, C. W., and D. A. Wright (1984), A Model for Generating Daily Weather Variables, technical report, U. S. Dept. of Agric., Agric. Res. Serv., Washington, D. C.

Rodenbeck, C., S. Houwelling, M. Gloor, and M. Heimann (2003), CO_2 flux history 1982–2001 inferred from atmospheric data using a global inversion of atmospheric transport, *Atmos. Chem. Phys.*, *3*, 1919–1964.

Rustad, L. E., J. L. Campbell, G. M. Marion, R. J. Norby, M. J. Mitchell, A. E. Hartley, J. H. C. Cornelissen, and J. Gurevitch (2001), A meta-analysis of the response of soil respiration, net nitrogen mineralization, and above-ground plant growth to experimental ecosystem warming, *Oecologia*, *126*, 543–562, doi:10.1007/s004420000544.

Schaefer, K., et al. (2002), Effect of climate on interannual variability of terrestrial CO_2 fluxes, *Global Biogeochem. Cycles*, *16*(4), 1102, doi:10.1029/2002GB001928.

Sitch, S., et al. (2003), Evaluation of ecosystem dynamics, plant geography and terrestrial carbon cycling in the LPJ dynamic global vegetation model, *Global Change Biol.*, *9*, 161–185, doi:10.1046/j.1365-2486.2003.00569.x.

Sitch, S., V. Brovkin, W. von Bloh, D. van Vuuren, B. Eickhout, and A. Ganopolski (2005), Impacts of future land cover changes on atmospheric CO_2 and climate, *Global Biogeochem. Cycles*, *19*, GB2013, doi:10.1029/2004GB002311.

Sitch, S., P. M. Cox, W. J. Collins, and C. Huntingford (2007), Indirect radiative forcing of climate change through ozone effects on the land-carbon sink, *Nature*, *448*, 791–794, doi:10.1038/nature06059.

Sitch, S., et al. (2008), Evaluation of the terrestrial carbon cycle, future plant geography and climate-carbon cycle feedbacks using five Dynamic Global Vegetation Models (DGVMs), *Global Change Biol.*, *14*, 2015–2039, doi:10.1111/j.1365-2486.2008.01626.x.

Slayback, D. A., J. E. Pinzon, S. O. Los, and C. J. Tucker (2003), Northern Hemisphere photosynthetic trends 1982–99, *Global Change Biol.*, *9*, 1–15, doi:10.1046/j.1365-2486.2003.00507.x.

Stephens, B. B., et al. (2007), Weak northern and strong tropical land carbon uptake from vertical profiles of atmospheric CO2, *Science*, *316*, 1732–1735, doi:10.1126/science.1137004.

Sutton, M. A., D. Simpson, P. E. Levy, R. I. Smith, S. Reis, M. van Oijen, and W. deVries (2008), Uncertainties in the relationship between atmospheric nitrogen deposition and forest carbon sequestration, *Global Change Biol.*, *14*, 2057–2063, doi:10.1111/j.1365-2486.2008.01636.x.

Tucker, C. J., J. E. Pinzon, M. E. Brown, D. A. Slayback, E. W. Pak, R. Mahoney, E. F. Vermote, and N. Saleous (2005), An extended AVHRR 8-km NDVI dataset compatible with MODIS and SPOT vegetation NDVI data, *Int. J. Remote Sens.*, *26*, 4485–4498, doi:10.1080/01431160500168686.

Valentini, R., et al. (2000), Respiration as the main determinant of carbon balance in European forests, *Nature*, *404*, 861–865, doi:10.1038/35009084.

Vuichard, N., P. Ciais, L. Belelli, P. Smith, and R. Valentini (2008), Carbon sequestration due to the abandonment of agriculture in the former USSR since 1990, *Global Biogeochem. Cycles*, *22*, GB4018, doi:10.1029/2008GB003212. (Correction, *Global Biogeochem. Cycles*, *23*, GB1004, doi:10.1029/2009GB003466.)

Vukicevic, T., B. H. Braswell, and D. Schimel (2001), A diagnostic study of temperature controls on global terrestrial carbon exchange, *Tellus, Ser. B*, *53*, 150–170, doi:10.1034/j.1600-0889.2001.d01-13.x.

Zeng, N., H. Qian, C. Roedenbeck, and M. Heimann (2005), Impact of 1998–2002 midlatitude drought and warming on terrestrial ecosystem and the global carbon cycle, *Geophys. Res. Lett.*, *32*, L22709, doi:10.1029/2005GL024607.

Zhou, L. M., C. J. Tucker, R. K. Kaufmann, D. Slayback, N. V. Shabanov, and R. B. Myneni (2001), Variations in northern vegetation activity inferred from satellite data of vegetation index during 1981 to 1999, *J. Geophys. Res.*, *106*, 20,069–20,083, doi:10.1029/2000JD000115.

P. Cadule, P. Ciais, P. Friedlingstein, N. de Noblet-Ducoudré, and N. Viovy, LSCE, UMR CEA, CNRS, Bat. 709, CE, L'Orme des Merisiers, F-91191 Gif-sur-Yvette, France.

S. Piao and T. Wang, Department of Ecology, College of Urban and Environmental Science, Peking University, Beijing 100871, China. (slpiao@pku.edu.cn)